 CMES, vol.23, no.1, pp.1-12, 2008

A Class of Wavelet-based Flat Shell Elements Using B-spline Wavelet on the Interval and Its applications

Xiang Jiawei[1], Chen Xuefeng[2], Yang Lianfa[3] and He Zhengjia[4]

Abstract: A class of flat shell elements is constructed by using the scaling functions of two-dimensional tensor product B-spline wavelet on the interval (BSWI). Unlike the process of direct wavelets adding in the wavelet Galerkin method, the element displacement field represented by the coefficients of wavelets expansions was transformed from wavelet space into physical space via the constructed two-dimensional transformation matrix. Then, the BSWI flat shell element is constructed by the assembly of BSWI plane elastomechanics and Mindlin plate elements. Because of the good character of BSWI scaling functions, the BSWI flat shell element combine the accuracy of B-spline functions approximation and various wavelet-based elements for structural analysis. Some static and dynamic numerical examples are studied to demonstrate the present element with higher efficiency and precision than the traditional element.

Keyword: B-spline wavelet on the interval, Wavelet-based element, Flat shell element, Folded plate, Shell

1 Introduction

High performance computing is an essential issue for some numerical simulation problems in civil and mechanical engineering. Some new numerical methods have been developed in recent years [Atluri, Liu and Han(2006a, 2006b); Han and Liu et al. (2006); Parussini (2007)], such as Meshless local Petrov-Galerkin (MLPG) mixed collocation method, Meshless local Petrov-Galerkin (MLPG) mixed finite difference method and fictitious domain approach for spectral/hp element method etc. The wavelet-based numerical analysis is also a new method developed in recent years. It can be viewed as a method in which the approximation functions are defined by the scaling or wavelet functions, similar to those used in signal and image processing [Cohen (2003)]. The desirable advantages of wavelet-based numerical method are multi-resolution properties and various basis functions for structural analysis. By means of "two-scale relations" of scaling functions, we can change the adopted scaling functions freely according to analytical requirements to improve solving precision. So the method is well argued by many researchers not only in numerical analysis domains [Dahmen (2001); Canuto, Tabacco and Urban (1999, 2000); Dahlke and Dahmen et al. (1997)] but also in structural analysis fields [Ko et al. (1995); Chen and Wu (1995, 1996a, 1996b); Zhou et al. (1998); Basu et al. (2003); Ma and He et al. (2003); Chen and He et al. (2004); Han and Ren et al. (2005); Mitra and Gopalakrishnan (2006); Xiang and Chen et al. (2006a, 2006b, 2007); He and Chen et al. (2005)]. Cohen proposed the adaptive wavelet methods framework for the numerical treatment of partial differential equations (PDEs) but failed to deal with the complex boundary conditions [Cohen (2003)]. Dahmen discussed the development of wavelet-based methods for PDEs and pointed out some of the important challenges which remain in this area [Dahmen (2001)]. Canuto, Tabacco and Urban demonstrated the possibility for the construction of wavelet-based element [Canuto, Tabacco and

[1] School of Mechantronic Engineering, Guilin University of Electronic Technology, Guilin, P.R.C.
[2] School of Mechanical Engineering, Xi'an Jiaotong University, Xi'an, P.R.C.
[3] School of Mechantronic Engineering, Guilin University of Electronic Technology, Guilin, P.R.C.
[4] School of Mechanical Engineering, Xi'an Jiaotong University, Xi'an, P.R.C.

Urban (1999, 2000)]. The wavelet-based numerical method was proved to converge for a wide class of elliptic operator equations including in particular differential operators as well as singular integral operators by Dahlke and Dahmen et al. [Dahlke and Dahmen et al. (1997)]. Ko et al constructed a class of one-dimensional wavelet-based element by using orthonormal, compactly supported Daubechies wavelets [Ko et al. (1995)]. Chen and Wu proposed wavelet-based elements using spline wavelet for the vibration analysis of frame and membrane structures with high performance [Chen and Wu (1995, 1996a, 1996b)]. Zhou proposed wavelet-based Galerkin method to bending analysis of beam and plate structures but cannot be applied easily as finite element method [Zhou et al. (1998)]. Basu indicated that the finite difference and Ritz type methods of the pre-computer era had largely been replaced in the computer era by FEM, boundary element method (BEM), Meshless method, and in the near future it might be the turn for wavelet method [Basu et al. (2003)].

Recently, one-dimensional Daubechies wavelet Euler beam element had been constructed by Ma [Ma and He et al. (2003)]. The two-dimensional Daubechies wavelet element for thin plate-bending problems had also been constructed by Chen [Chen and He et al. (2004)]. However, for discrete wavelets lacking of the explicit function expression, traditional numerical integrals such as Gauss integrals cannot provide desirable precision, the key problem is to calculate connection coefficients [Ma and He et al. (2003); Chen and He et al. (2004)]. Since the connection coefficients derivation can only be obtained for integration in global coordinates, it will fail when the integrand involves variant Jacobians. Moreover, the connection coefficients calculation is a complex process, which will increases the coding work and calculating costs [Chen and Wu (1996a)]. Han and Ren et al. extended the wavelet-based finite element method to thick plate by using mixed variational principle [Han and Ren et al. (2005)]. Mitra and Gopalakrishnan proposed a 2-D wavelet based spectral finite element (WSFE) to study wave propagation in an isotropic plate [Mitra and Gopalakrishnan (2006)]. Xiang and Chen et al. successfully constructed classes of 1D wavelet-based elements, plane elastomechanics and Mindlin plate elements and truncated conical shell elements by using B-spline wavelet on the interval [Xiang and Chen et al. (2006a, 2006b, 2007)]. He summarized the advanced in theory study and engineering application of wavelet finite element [He and Chen et al. (2005)].

In the construction of wavelet-based element, instead of traditional polynomial interpolation, scaling or wavelet functions have been adopted to form the shape function, which embodied with the prominent advantage that the semi-orthogonal BSWI have explicit expressions. Therefore, the element stiffness and mass matrices can be calculated conveniently. Furthermore, B-spline wavelets have the best approximation properties among all known wavelets of a given order L [Wang (1996)]. However, the originally spline wavelets are defined on the whole real space. Using the wavelets defined on the whole real space as interpolating functions will bring the numerical instability phenomenon [Bertoluzza, Naldi and Ravel. (1994)]. To overcome this limitation, Chui and Quak et al. [Chui and Quak (1992); Quak and Weyrichm (1994)] constructed BSWI and presented the corresponding fast decomposition and reconstruction algorithm. Goswami and Chui et al. also used the BSWI solving the first-kind integral equations [Goswami, Chan and Chui. (1995)]. The wavelets on a bounded interval have limited dimension towards every scaling and wavelet space. So any functions on the interval can be expanded as a sum of finite-dimensional wavelet series, which plays a very important role in constructing element interpolating (or shape) functions [Jia, Wang and Zhou (2003)]. Moreover, because there are more nodes in each BSWI element than traditional one, fewer BSWI elements are needed than traditional ones to get the same accuracy. However, wavelet-based finite element method is always used in wavelet space, and the wavelet coefficients are used as its degree of freedoms (DOFs). In this way, when a complex structure is analyzed, it becomes very difficult that neighboring element or

different classes of elements are connected. At the same time, boundary conditions cannot be processed simply as done in traditional element. These shortcomings limit the wide applications of wavelet-based FEM. So the transformation matrix [Xiang, Chen and He et al. (2006a, 2006b, 2007)] is introduced to benefit the connection of the constructed C_0 and C_1 type BSWI elements.

Flat shell elements are used extensively in engineering practice for the simplicity of the formulation, the effectiveness of the computation and the flexibility in applications (shells and folded plate structures). In this paper, we used BSWI scaling functions as interpolation functions to construct BSWI plane elastomechanics and Mindlin plate elements via the constructed element transformation matrix. Therefore, a class of BSWI flat shell element is constructed by the assembly of BSWI plane elastomechanics and Mindlin plate elements.

The outline of this paper is as follows. In Section 2, we present a brief introduction of the basic theory of BSWI scaling functions and wavelets. In Section 3, BSWI plane elastomechanics and Mindlin plate elements are constructed by introducing the C_0 type element transformation matrix and then assembled them directly to generate BSWI flat shell element. Section 4 provides some numerical examples which demonstrate the accuracy and efficiency of the constructed BSWI flat shell element.

2 Two-dimensional BSWI tensor product scale functions

B-splines for a given simple knot sequence can be constructed by taking piecewise polynomials between the knots and joining them together at the knots in such a way as to obtain a certain order of overall smoothness. B-splines of order m are in C^{m-2}. Since the function $f(x)$ on the interval $[a,\ b]$ can be transferred to the interval [0, 1] by the transformation formula $\xi = (x-a)/(b-a)$, it only needs to construct mth order B-spline space on the interval [0, 1]. Generally, the interval [0, 1] can be divided into 2^j, ($j \in \mathbf{Z}^+$ is the scale) segments, and then increasing m-1 knots outside each endpoint and looking the two lateral $m-1$ knots as multiple knots of the endpoint 0 and 1. Let $\{\xi_k^j\}_{k=-m+1}^{2^j+m-1}$ be a knot sequence with m-multiple knots at 0 and 1, then the whole knot number is 2^j+2m-1, and the knot sequence form B-spline functions, which can be further constructed to the mth order nested B-spline subspace $V_j^{[0,\,1]}$. Its basis functions are given below

$$\begin{aligned} &B_{m,k}^j(x) = N_m\left(2^j\xi - k\right); \\ &\qquad\qquad \text{for } k = -m+1,\cdots,2^j-1; \\ &\text{supp}B_{m,k}^j = \left[\xi_k^j, \xi_{m+k}^j\right] \end{aligned} \tag{1}$$

where $N_m(x)$ is cardinal splines. Let $\phi_{m,k}^j(\xi) = B_{m,k}^j(\xi)$ be the scaling functions of BSWI, we can obtain the multi-resolution analysis (MRA) on the bounded interval [0, 1] [Chui and Quak (1992); Quak and Weyrichm (1994)]. The smoothness order of scaling functions $\phi_{m,k}^j(\xi)$ is $m-1$.

The support of the inner (without multiple knots) B-splines occupies m segments and that of the corresponding semi-orthogonal (SO) wavelet occupies $2m$-1 segments. At any scale j, the discretization step is $1/2^j$ which, for $j>0$, gives 2^j number of segments on [0, 1]. Therefore, to have at least one inner wavelet on the interval [0, 1], the following condition must be satisfied

$$2^j \geq 2m-1 \tag{2}$$

While 0 scale mth order B-spline functions and the corresponding wavelets [Goswami, Chan and Chui. (1995)] are given, j scale mth order BSWI (simplely denoted as BSWIm_j) scaling functions $\phi_{m,k}^j(\xi)$and the corresponding wavelets $\psi_{m,k}^j(\xi)$ can be evaluated by the following formula

$$\phi_{m,k}^j(\xi) = \begin{cases} \phi_{m,k}^l(2^{j-l}\xi); & k=-m+1,\cdots,-1 \\ \phi_{m,2^j-m-k}^l(1-2^{j-l}\xi); & k=2^j-m+1,\cdots,2^j-1 \\ \phi_{m,0}^l(2^{j-l}\xi-2^{-l}k); & k=0,\cdots,2^j-m \end{cases} \begin{matrix} \text{(0 boundary scaling fuctions)} \\ \text{(1 boundary scaling fuctions)} \\ \text{(inner scaling fuctions)} \end{matrix} \tag{3}$$

$$\psi_{m,k}^j(\xi) =$$

$$\begin{cases} \psi^l_{m,k}(2^{j-l}\xi); & k=-m+1,\cdots,-1 \\ \psi^l_{m,2^j-2m-k+1}\left(1-2^{j-l}\xi\right); & k=2^j-2m+2,\cdots \\ & \qquad \cdots,2^j-m \\ \psi^l_{m,0}\left(2^{j-l}\xi-2^{-l}k\right); & k=0,\cdots,2^j-2m+1 \end{cases} \begin{matrix} \text{(0 boundary wavelets)} \\ \text{(1 boundary wavelets)} \\ \text{(inner wavelets)} \end{matrix} \quad (4)$$

The wavelets compactly supported intervals are

$$\text{supp}\psi^j_{m,k}(\xi) = \begin{cases} \left[0,\ (2m-1+k)2^{-j}\right] \\ \left[k2^{-j},\ 1\right] \\ \left[k2^{-j},\ (2m-1+k)2^{-j}\right] \end{cases} \quad (5)$$

Let j_0 be the scale for which the condition Eq. (2) is satisfied. Then for each $j > j_0$, let $l = 0$, we can get the scaling and wavelet functions easily through Eq. (3) and Eq. (4). There are $m-1$ boundary scaling functions and wavelets at 0 and 1, $2^j - m + 1$ inner scaling functions, and $2^j - 2m + 2$ inner wavelets. Fig. 1(a) and Fig.1(b) shows all the scaling functions of BSWI4_2 and BSWI4_3, respectively.

Tensor product of one-dimensional wavelets [Mallat (1999)] is the easy and direct way to construct two-dimensional BSWI. A semi-orthonormal wavelet basis at scale j of $L^2(\mathbf{R}^2)$ is constructed with tensor product of the one-dimensional MRA approximation space V^1_j and V^2_j. Tensor product subspace $F_j = V^1_j \otimes V^2_j \subset L^2(\mathbf{R}^2)$ (For BSWI, the initial scale is j_0).

When the one-dimensional BSWIm_j scaling functions are employed to form the two-dimensional tensor product wavelet on the interval, the scaling functions are

$$\boldsymbol{\phi} = \boldsymbol{\phi}_1 \otimes \boldsymbol{\phi}_2 \quad (6)$$

where

$$\boldsymbol{\phi}_1 = \left\{\phi^j_{m,-m+1}(\xi)\ \ \phi^j_{m,-m+2}(\xi)\ \cdots\ \phi^j_{m,2^j-1}(\xi)\right\}$$

is the row vector combined by the scaling functions for m at the scale j.

$$\boldsymbol{\phi}_2 = \left\{\phi^j_{m,-m+1}(\eta)\ \ \phi^j_{m,-m+2}(\eta)\ \cdots\ \phi^j_{m,2^j-1}(\eta)\right\}$$

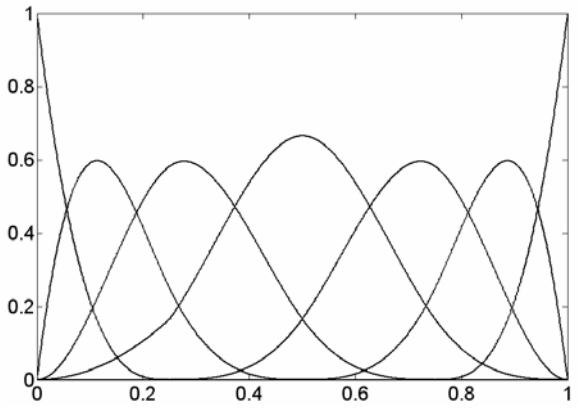

(a) BSWI4_2 scaling functions on the interval [0, 1]

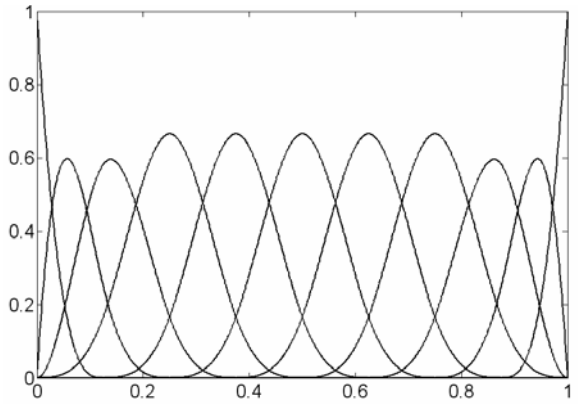

(b) BSWI4_3 scaling functions on the interval [0, 1]

Figure 1: One dimensional BSWI scaling functions

is the row vector combined by the one-dimensional BSWIm_j scaling functions. $\otimes$ is the kronecker symbol.

The wavelets are $\boldsymbol{\psi}^1 = \boldsymbol{\phi}_1 \otimes \boldsymbol{\psi}_2$, $\boldsymbol{\psi}^2 = \boldsymbol{\psi}_1 \otimes \boldsymbol{\phi}_2$ and $\boldsymbol{\psi}^3 = \boldsymbol{\psi}_1 \otimes \boldsymbol{\psi}_2$. Fig. 2(a) shows all the tensor product BSWI scaling functions, which are generated by the one-dimensional BSWI4_3 scaling functions. The two-dimensional BSWI scaling functions that generated by one-dimensional BSWI2_2 is shown in Fig. 2(b).

3 BSWI flat shell element

For many practical purposes, the flat element approximation gives very adequate answers. Indeed in many practical problems the structure is in fact composed of flat surfaces especially for folded plate structure. BSWI flat shell ele-

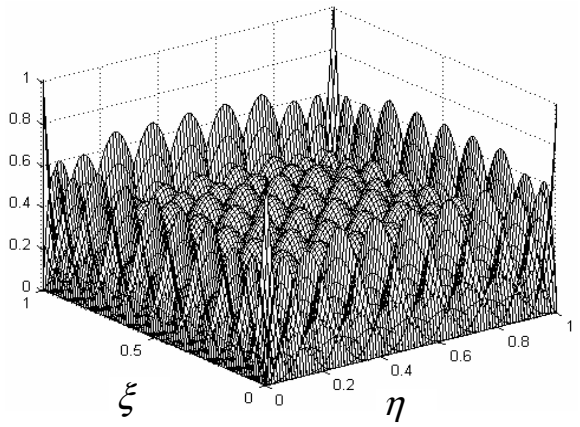

(a) Two-dimensional BSWI4$_3$ scaling functions

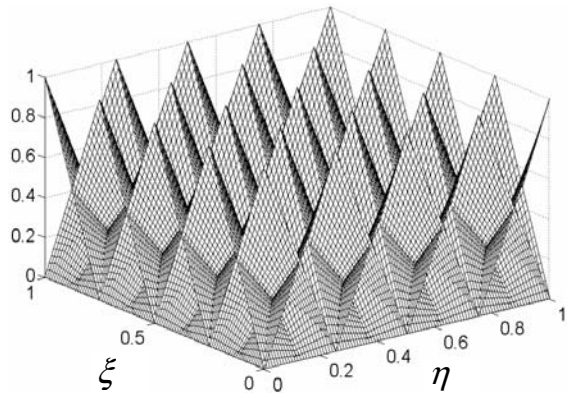

(b) Two-dimensional BSWI4$_2$ scaling functions

Figure 2: Tensor product BSWI scaling functions $\boldsymbol{\phi} = \phi^1 \otimes \phi^2$

ment can be constructed by combining the BSWI plane elastomechanics and Mindlin plate elements [Zienkiewicz and Taylor (1988)].

Fig.3 shows the layout of BSWI flat shell element nodes and the corresponding degree of freedoms (DOFs). l_{ex} and l_{ey} denote the element length. The element possesses $(n+1)^2$ (where, $n = 2^j + m - 1$) nodes. At each node i (where, $i = 1, 2, \cdots, n^2$), three displacements and two rotations will be prescribed, i.e. $u_i, v_i, w_i, \theta_{ix}, \theta_{iy}$. In order to transform element matrix from the local coordinate to global coordinate, the rotation θ_{iz} is consider and the corresponding element stiffness and mass matrices and loading column vector will be modified by inserting an appropriate number of zeros. So the element physical DOFs in the local system are

$$\mathbf{a}^e = \Big\{ u_1 \;\; v_1 \;\; w_1 \;\; \theta_{1x} \;\; \theta_{1y} \;\; \theta_{1z} \cdots u_{n+1} \;\; v_{n+1} \;\; w_{n+1} \;\; \theta_{(n+1)x} \;\; \theta_{(n+1)y} \;\; \theta_{(n+1)z} \Big\}^\top \quad (7)$$

and the total nodal DOFs are $6n^2$.

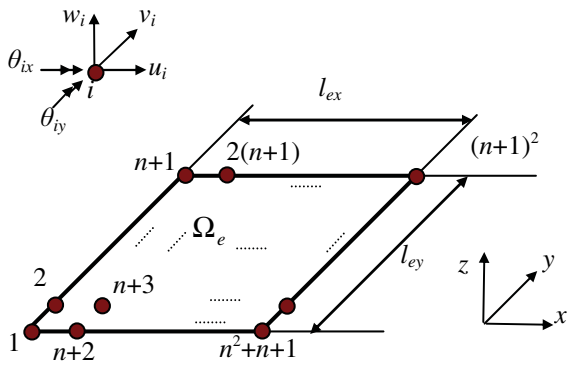

Figure 3: BSWI flat shell element on the element solving domain Ω_e

BSWI flat shell element stiffness matrix is now made up of the following sub-matrices

$$\mathbf{K}^e_{p,q} = \left[\begin{array}{cc:ccc:c} \multicolumn{2}{c:}{\multirow{2}{*}{$\mathbf{K}^{(m)}_{p,q}$}} & 0 & 0 & 0 & 0 \\ & & 0 & 0 & 0 & 0 \\ \hdashline 0 & 0 & \multicolumn{3}{c:}{\multirow{3}{*}{$\mathbf{K}^{(b)}_{p,q}$}} & 0 \\ 0 & 0 & & & & 0 \\ 0 & 0 & & & & 0 \\ \hdashline 0 & 0 & 0 & 0 & 0 & 0 \end{array}\right]; \quad \text{for } p, q = 1, \cdots, (n+1)^2 \quad (8)$$

where (m) denotes membrane stress situations and (b) denotes bending stress situations. In order to describe the insignificant parameter θ_{iz}, we insert one row and one column vectors in the element stiffness sub-matrices $\mathbf{K}^e_{p,q}$ respectively.

To describe simply, the exterior bending moments are neglected and the loading column vector can be written by

$$\mathbf{P}^e_i = \left\{ p_{u,i} \;\; p_{v,i} \;\vdots\; p_{w,i} \;\; 0 \;\; 0 \;\vdots\; 0 \right\}^\top \quad (9)$$

The above formulation is validity for any shape of quadrilateral element which can be mapped

to standard rectangle element by using isoparametric transformation [Zienkiewicz and Taylor (1988)].

BSWI plane elastomechanics element solving equations are [Xiang and Chen et al. (2006a)]

$$\mathbf{K}^{(m)}\mathbf{a}^{(m)} = \mathbf{P}^{(m)} \tag{10}$$

where

$$\mathbf{a}^{(m)} = \left\{u_1 \ v_1 \ u_2 \ v_2 \ \cdots \ u_{(n+1)^2} \ v_{(n+1)^2}\right\}^{\top} \tag{11}$$

$$\mathbf{P}^{(m)} = \left\{p_{u,1} \ p_{v,1} \ p_{u,2} \ p_{v,2} \ \cdots \ p_{u,(n+1)^2} \ p_{v,(n+1)^2}\right\}^{\top} \tag{12}$$

$$\mathbf{K}_{p,q}^{(m)} = \begin{bmatrix} k_{p,q}^{e,1} & k_{p,q}^{e,2} \\ k_{p,q}^{e,3} & k_{p,q}^{e,4} \end{bmatrix} \tag{13}$$

in which the element stiffness submatrices and loading vector can be solved by the following formulae

$$\mathbf{P}_u = ((\mathbf{R}^e)^{-1})^{\top}\left\{\int_{S_\sigma} p_x\boldsymbol{\phi}^{\top}\mathrm{d}s + \int_{\Omega_e} f_x\boldsymbol{\phi}^{\top}\mathrm{d}\Omega_e\right\}$$

$$\mathbf{P}_v = ((\mathbf{R}^e)^{-1})^{\top}\left\{\int_{S_\sigma} p_y\boldsymbol{\phi}^{\top}\mathrm{d}s + \int_{\Omega_e} f_y\boldsymbol{\phi}^{\top}\mathrm{d}\Omega_e\right\}$$

$$\mathbf{K}^{e,1} = \frac{E}{1-\mu^2}\left\{\mathbf{A}_1^{11}\otimes\mathbf{A}_2^{00} + \frac{1-\mu}{2}\mathbf{A}_1^{00}\otimes\mathbf{A}_2^{11}\right\}$$

$$\mathbf{K}^{e,2} = \frac{E}{1-\mu^2}\left\{\mu\mathbf{A}_1^{10}\otimes\mathbf{A}_2^{01} + \frac{1-\mu}{2}\mathbf{A}_1^{01}\otimes\mathbf{A}_2^{10}\right\}$$

$$\mathbf{K}^{e,3} = \left(\mathbf{K}^{e,2}\right)^{\top}$$

$$\mathbf{K}^{e,4} = \frac{E}{1-\mu^2}\left\{\mathbf{A}_1^{00}\otimes\mathbf{A}_2^{11} + \frac{1-\mu}{2}\mathbf{A}_1^{11}\otimes\mathbf{A}_2^{00}\right\}$$

$$\mathbf{A}_1^{00} = \left[(\mathbf{T}_1^e)^{-1}\right]^{\top}\left\{l_{ex}\int_0^1 (\boldsymbol{\phi}_1)^{\top}\boldsymbol{\phi}_1\mathrm{d}\xi\right\}(\mathbf{T}_1^e)^{-1}$$

$$\mathbf{A}_1^{01} = \left[(\mathbf{T}_1^e)^{-1}\right]^{\top}\left\{\int_0^1 (\boldsymbol{\phi}_1)^{\top}\frac{\mathrm{d}\boldsymbol{\phi}_1}{\mathrm{d}\xi}\mathrm{d}\xi\right\}(\mathbf{T}_1^e)^{-1}$$

$$\mathbf{A}_1^{10} = \left[(\mathbf{T}_1^e)^{-1}\right]^{\top}\left\{l_{ex}\int_0^1 \left(\frac{\mathrm{d}\boldsymbol{\phi}_1}{\mathrm{d}\xi}\right)^{\top}\boldsymbol{\phi}_1\mathrm{d}\xi\right\}(\mathbf{T}_1^e)^{-1}$$

$$\mathbf{A}_1^{11} = \left[(\mathbf{T}_1^e)^{-1}\right]^{\top}\left\{\frac{1}{l_{ex}}\int_0^1 \left(\frac{\mathrm{d}\boldsymbol{\phi}_1}{\mathrm{d}\xi}\right)^{\top}\frac{\mathrm{d}\boldsymbol{\phi}_1}{\mathrm{d}\xi}\mathrm{d}\xi\right\}(\mathbf{T}_1^e)^{-1}$$

A_2^{ij} $(i,j=0,1)$ are similar to A_1^{ij} $(i,j=0,1)$ if l_{ex}, $d\xi$ and $\mathbf{T}_1^e$ are replaced by l_{ey}, $d\eta$ and $\mathbf{T}_2^e$ respectively. μ denotes possion's ratio, E denotes Yang's modulus, $\mathbf{f} = \{f_x \ f_y\}^{\top}$ is the column vector of body forces, and $\mathbf{p} = \{p_x \ p_y\}^{\top}$ is the column vector of surface tractions in the x and y directions.

The C_0 type element transformation matrix is given by

$$\mathbf{R}^e = \mathbf{T}_1^e \otimes \mathbf{T}_2^e \tag{14}$$

where

$$\begin{cases} \mathbf{T}_1^e = \{\boldsymbol{\phi}_1^{\top}(\xi_1)\ \boldsymbol{\phi}_1^{\top}(\xi_2)\ldots\ \boldsymbol{\phi}_1^{\top}(\xi_{n+1})\}^{\top} \\ \mathbf{T}_2^e = \{\boldsymbol{\phi}_2^{\top}(\eta_1)\ \boldsymbol{\phi}^{\top}(\eta_2)\ldots\boldsymbol{\phi}_2^{\top}(\eta_{n+1})\}^{\top} \end{cases} \tag{15}$$

Similarly to BSWI plane elastomechanics element, BSWI Mindlin plate element solving equations can be given by[Xiang and Chen et al. (2006a)]

$$\mathbf{K}^{(b)}\mathbf{a}^{(b)} = \mathbf{P}^{(b)} \tag{16}$$

where

$$\mathbf{a}^{(b)} = \left\{w_1 \ \theta_{1x} \ \theta_{1y} \ \cdots \ w_{n+1} \ \theta_{(n+1)^2x} \ \theta_{(n+1)^2y}\right\}^{\top} \tag{17}$$

$$\mathbf{P}^{(b)} = \left\{p_{w,1} \ 0 \ 0 \ p_{w,2} \ 0 \ 0 \ \cdots \ p_{w,(n+1)^2} \ 0 \ 0\right\}^{\top} \tag{18}$$

$$\mathbf{K}_{p,q}^{(b)} = \begin{bmatrix} k_{p,q}^{e,1} & k_{p,q}^{e,2} & k_{p,q}^{e,3} \\ k_{p,q}^{e,4} & k_{p,q}^{e,5} & k_{p,q}^{e,6} \\ k_{p,q}^{e,7} & k_{p,q}^{e,8} & k_{p,q}^{e,9} \end{bmatrix}; \quad \text{for } p,q = 1,\cdots,(n+1)^2 \tag{19}$$

in which the element stiffness submatrices and loading vector can be solved by the following for-

mulae

$$
\begin{aligned}
\mathbf{P}_w &= \left[(\mathbf{R}^e)^{-1}\right]^\top l_{ex} l_{ey} \int_0^1 \int_0^1 q(\xi,\eta)\boldsymbol{\phi}^\top \mathrm{d}\xi \mathrm{d}\eta \\
\mathbf{K}^{e,1} &= C_0 \left\{ \mathbf{A}_1^{1,1} \otimes \mathbf{A}_2^{0,0} + \mathbf{A}_1^{0,0} \otimes \mathbf{A}_2^{1,1} \right\} \\
\mathbf{K}^{e,2} &= -C_0 \mathbf{A}_1^{1,0} \otimes \mathbf{A}_2^{0,0} \\
\mathbf{K}^{e,3} &= -C_0 \mathbf{A}_1^{0,0} \otimes \mathbf{A}_2^{1,0} \\
\mathbf{K}^{e,4} &= \left(\mathbf{K}^{e,2}\right)^\top \\
\mathbf{K}^{e,5} &= D_0 \left\{ \mathbf{A}_1^{1,1} \otimes \mathbf{A}_2^{0,0} + \frac{1-\mu}{2} \mathbf{A}_1^{0,0} \otimes \mathbf{A}_2^{1,1} \right\} \\
&\quad + C_0 \mathbf{A}_1^{0,0} \otimes \mathbf{A}_2^{0,0} \\
\mathbf{K}^{e,6} &= D_0 \left\{ \mu \mathbf{A}_1^{1,0} \otimes \mathbf{A}_2^{0,1} + \frac{1-\mu}{2} \mathbf{A}_1^{0,1} \otimes \mathbf{A}_2^{1,0} \right\} \\
\mathbf{K}^{e,7} &= \left(\mathbf{K}^{e,3}\right)^\top \\
\mathbf{K}^{e,8} &= \left(\mathbf{K}^{e,6}\right)^\top \\
\mathbf{K}^{e,9} &= D_0 \left\{ \mathbf{A}_1^{0,0} \otimes \mathbf{A}_2^{1,1} + \frac{1-\mu}{2} \mathbf{A}_1^{1,1} \otimes \mathbf{A}_2^{0,0} \right\} \\
&\quad + C_0 \mathbf{A}_1^{0,0} \otimes \mathbf{A}_2^{0,0}
\end{aligned}
$$

in which $\mathbf{A}_1^{ij}$ $(i,j=0,1)$ and $\mathbf{A}_2^{ij}$ $(i,j=0,1)$ are similar to Eq.(10), $D_0 = \frac{Et^3}{12(1-\mu^2)}$, $C_0 = \frac{5Et}{12(1+\mu)}$ and t is the thickness of shells.

The element stiffness matrix or loading column vector derived here used a system of local coordinates as the membrane and bending components are originally derived for this system. when the BSWI flat shell element is applied to solving engineering structure problems, element DOFs in local coordinates must have to transfer to a common global system to benefit the assembly of the elements.

The element physical DOFs in the global coordinate system are defined by

$$
\begin{aligned}
\overline{\mathbf{a}}^e = \Big\{ & \overline{u}_1 \ \overline{v}_1 \ \overline{w}_1 \ \overline{\theta}_{1x} \ \overline{\theta}_{1y} \ \overline{\theta}_{1z} \cdots \overline{u}_{n+1} \ \overline{v}_{n+1} \\
& \overline{w}_{n+1} \ \overline{\theta}_{(n+1)x} \ \overline{\theta}_{(n+1)y} \ \overline{\theta}_{(n+1)z} \Big\}^\top
\end{aligned} \tag{20}
$$

The transformation relationships between local and global coordinate systems are

$$
\overline{\mathbf{a}}^e = \mathbf{S}^\top \mathbf{a}^e, \quad \mathbf{a}^e = \mathbf{S}\overline{\mathbf{a}}^e \tag{21}
$$

where

$$
\mathbf{S} = \begin{bmatrix} L_1 & & & \\ & L_2 & & \\ & & \ddots & \\ & & & L_{(n+1)^2} \end{bmatrix} \tag{22}
$$

in which

$$
\mathbf{L}_l = \begin{bmatrix} \boldsymbol{\lambda} & 0 \\ 0 & \boldsymbol{\lambda} \end{bmatrix} \tag{23}
$$

and

$$
\boldsymbol{\lambda} = \begin{bmatrix} \lambda_{x\overline{x}} & \lambda_{x\overline{y}} & \lambda_{x\overline{z}} \\ \lambda_{y\overline{x}} & \lambda_{y\overline{y}} & \lambda_{y\overline{z}} \\ \lambda_{z\overline{x}} & \lambda_{z\overline{y}} & \lambda_{z\overline{z}} \end{bmatrix}; \quad \text{for } l = 1, \cdots, (n+1)^2 \tag{24}
$$

in which the direction cosine $\lambda_{x\overline{x}} = \cos(x,\overline{x})$, $\lambda_{x\overline{y}} = \cos(x,\overline{y})$ $\lambda_{x\overline{z}} = \cos(x,\overline{z})$, etc.

The element stiffness matrix and loading column vector in global coordinate system are now can be written by

$$
\overline{\mathbf{K}}^e \overline{\mathbf{a}}^e = \overline{\mathbf{P}}^e \tag{25}
$$

where

$$
\overline{\mathbf{K}}^e = \mathbf{S}^\top \mathbf{K}^e \mathbf{S} \tag{26}
$$

$$
\overline{\mathbf{P}}^e = \mathbf{S}^\top \mathbf{P}^e \tag{27}
$$

Assembling the element stiffness matrix and loading column vector in the common global coordinate system, we can achieve the final solution follow the standard pattern. The resulting displacements calculated are referred to the global system, and before the stresses can be computed it is necessary to change these for each element of the local system.

BSWI flat shell element free vibration frequency equations are

$$
\left| \mathbf{S}^\top \mathbf{K}^e \mathbf{S} - \omega^2 \mathbf{S}^\top \mathbf{M}^e \mathbf{S} \right| = 0 \tag{28}
$$

where the element mass matrix is given by

$$\mathbf{M}^e_{p,q} = \begin{bmatrix} \mathbf{M}^{(m)}_{p,q} & \begin{matrix} 0 & 0 & 0 \\ 0 & 0 & 0 \end{matrix} & \begin{matrix} 0 \\ 0 \end{matrix} \\ \begin{matrix} 0 & 0 \\ 0 & 0 \\ 0 & 0 \end{matrix} & \mathbf{M}^{(b)}_{p,q} & \begin{matrix} 0 \\ 0 \\ 0 \end{matrix} \\ \begin{matrix} 0 & 0 \end{matrix} & \begin{matrix} 0 & 0 & 0 \end{matrix} & 0 \end{bmatrix}; \quad p,q = 1,\cdots,(n+1)^2 \quad (29)$$

in which $\mathbf{M}^{(m)}$ and $\mathbf{M}^{(b)}$ are the element mass matrices of BSWI plane elastomechanics element and BSWI Mindlin plate element respectively, are given by

$$\mathbf{M}^{(m)}_{p,q} = \begin{bmatrix} \mathbf{M}_{p,q} & 0 \\ 0 & \mathbf{M}_{p,q} \end{bmatrix} \quad (30)$$

$$\mathbf{M}^{(b)}_{p,q} = \begin{bmatrix} \mathbf{M}_{p,q} & 0 & 0 \\ 0 & \mathbf{M}_{p,q} & 0 \\ 0 & 0 & \mathbf{M}_{p,q} \end{bmatrix} \quad (31)$$

where the element mass submatrices can be computed by

$$\mathbf{M} = \rho t \mathbf{A}^{00}_1 \otimes \mathbf{A}^{00}_2 \quad (32)$$

4 Numerical examples

In order to verify the validity and advantages of the presented BSWI flat shell element in the problems of plates and shells, four typical examples are illustrated. We adopt the BSWIm_j (where m is the order and j is the scale of BSWI scaling functions) plane elastomechanics and Mindlin plate elements to assemble BSWI flat shell element, and it is simply marked as BSWIm_j flat shell element. In order to describe simply, the units of all parameters are omitted.

Example 1 Fig.4 shows 1/4 square plate with hole subjected to uniform loading, the physical parameters and loading are shown in Fig.4. 2 BSWI4_3 flat shell elements (1386 DOFs) and 10×20 (1386 DOFs), 20×40 (5166 DOFs), 30×60 (11346DOFs) and 50×100(30906DOFs) SHELL63 (A common used element in commercial software ANSYS) elements are applied respectively to solve this plate. Fig 5 shows the relative errors at appointed sides with the nodal stress

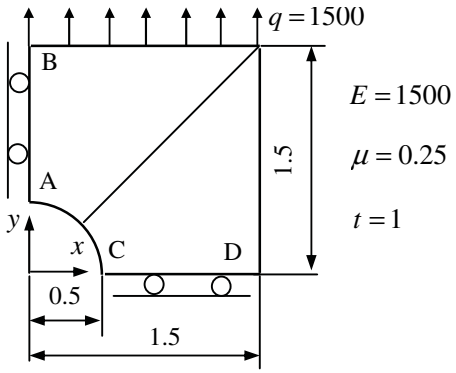

Figure 4: 1/4 square plate with hole subjected to uniform loading

results of 50×100 SHELL63 elements when 2 BSWI43 flat shell elements and 10×20, 20×40, 30×60 SHELL63 elements are applied to solve this example. Both the σ_x and σ_y relative errors of 2 BSWI4_3 flat shell elements are smaller than those of 30×60 SHELL63 elements and that the total DOFs of 2 BSWI43 flat shell elements far from those of the 30×60 SHELL63 elements. The results of this example indicate the accuracy and efficiency of the BSWI flat shell element.

Example 2 Fig.6 shows a folded plate structure subjected to uniform loading, the parameters and loading are $E = 2.06\times 10^{11}$, $L = 50$, $t = 1$, $r_2 = 100$, $\mu = 0.3$, $q = 1000$ and $\alpha = 30^0$ respectively. Both side AB and EF are free, and the other sides are simply supported.

2 BSWI4_3 flat shell elements (1386 DOFs) and 80×40 (19926 DOFs) SHELL63 elements are applied respectively to solve the folded plate structure. The displacements of appointed sides are shown in Fig 7. 2 BSWI4_3flat shell elements results are in good agree with the 80×40 SHELL63 elements.

Example 3 A folded shell structure modal analysis, the geometrical shape is shown in Fig.5. Material density $\rho = 7860$, both side AB and EF are clamped, and the other sides are free, and the other parameters are shown in Example 2.

2 BSWI4_3 flat shell elements (1386 DOFs) and 80×40(19926 DOFs) SHELL63 elements are ap-

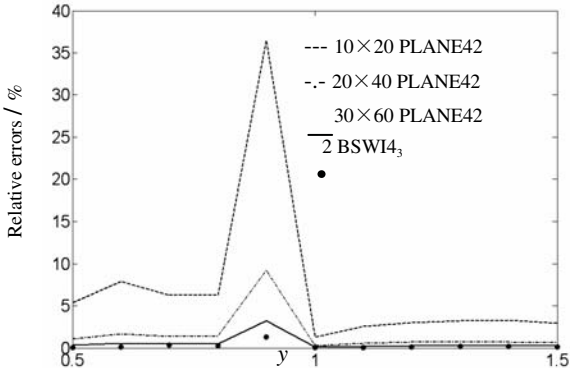

(a) Nodal stress σ_x relative errors at side AB

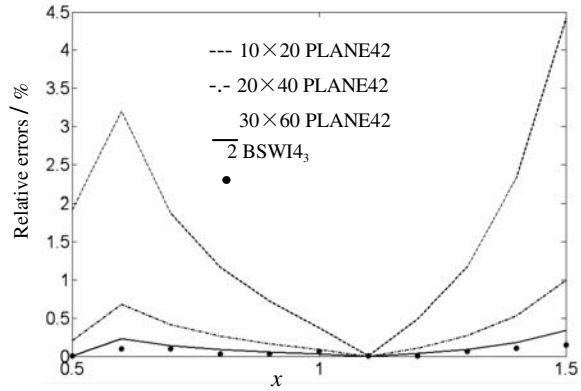

(b) Nodal stress σ_y relative errors at side CD

Figure 5: The relative nodal stresses errors with 50×100 shell63 elements on appointed sides

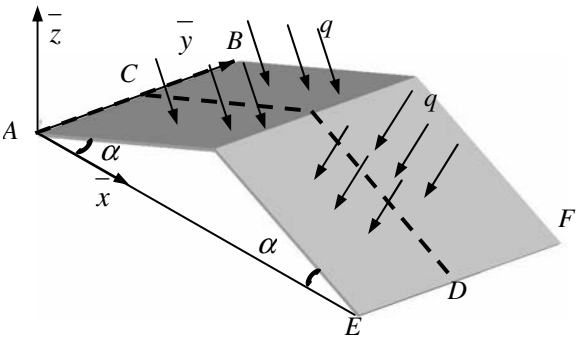

Figure 6: Folded plate structure subjected to uniform loading q

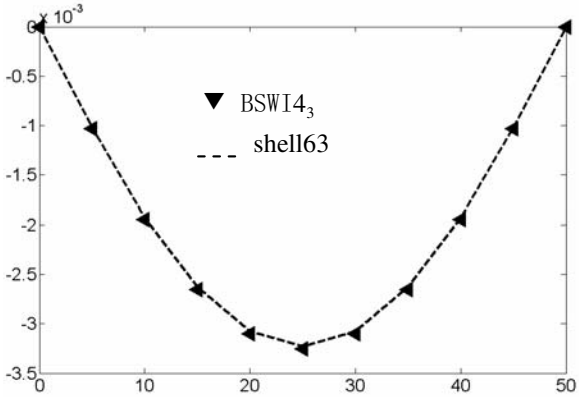

(a) $\overline{w}$ side AB

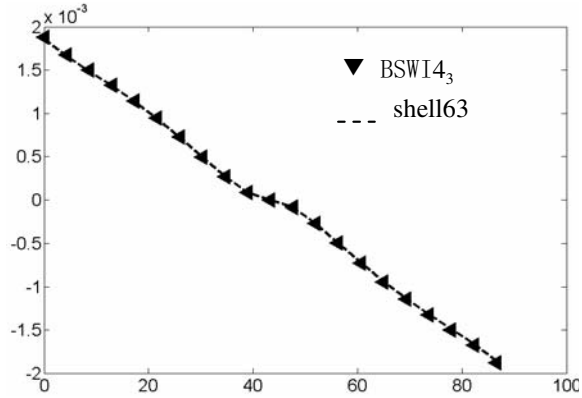

(b) $\overline{u}$ side CD

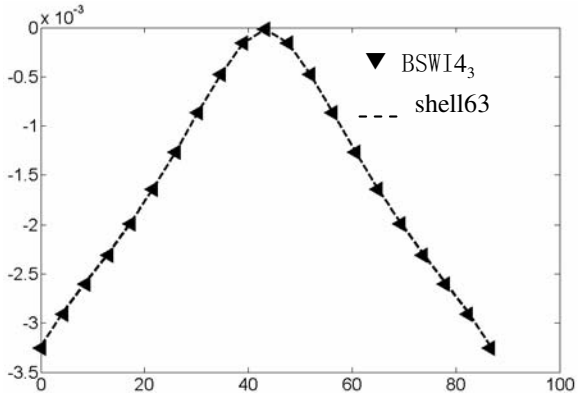

(c) $\overline{w}$ side CD

Figure 7: Displacement of the appoint sides

Table 1: Comparison of the frequencies between 80×40 SHELL63 and 2 BSWI4$_3$ elements (Hz)

Method	f_1	f_2	f_3	f_4	f_5
SHELL63	1.4982	2.0301	2.1755	2.5863	3.9178
BSWI4$_3$	1.4923	2.0143	2.1646	2.5635	3.8571
Error/ %	0.394	0.778	0.501	0.882	1.549
Method	f_6	f_7	f_8	f_9	f_{10}
SHELL63	4.2829	4.8748	5.5502	5.947	6.4991
BSWI4$_3$	4.2111	4.8235	5.4707	5.8808	6.4026
Error/ %	1.676	1.052	1.432	1.113	1.485

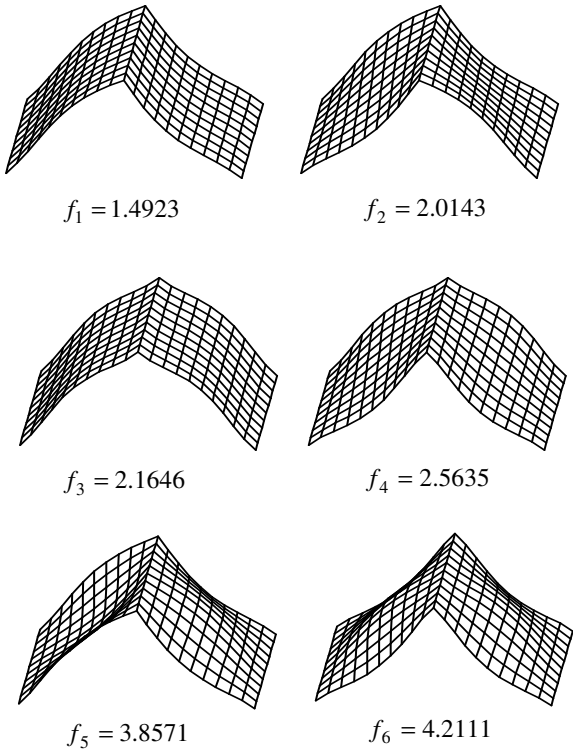

Figure 8: The first six mode shapes

plied respectively to the modal analysis of the folded plate structure. Tab.1 gives the first ten frequencies f_i $(i = 1, 2, \cdots, 10)$ solutions of both the 2 BSWI4$_3$ flat shell elements and 80×40 SHELL63 elements. And the relative errors of the two kinds of elements are also given in Tab.1. The small relative errors indicated that the constructed BSWI flat shell element can achieve high precision and efficiency not only in static but also in dynamic analysis fields. Fig.8 gives the first six mode shapes.

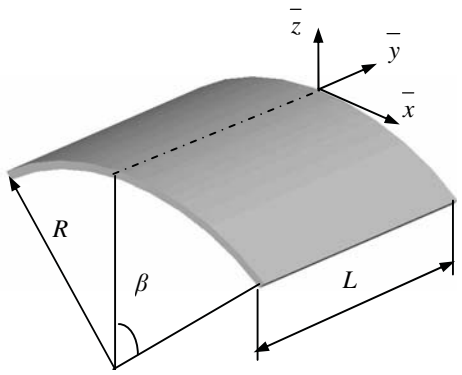

Figure 9: Simply supported cylindrical shell roof

Example 4 The modal analysis a simply supported cylindrical shell roof, the geometrical shape is shown in Fig.9. The parameters are $\rho = 1$, $L = 1$, $R = 1.91$, $t = 0.0191$, $E = 1$, $\mu = 0.3$, $\beta = 30^0$.

4 BSWI2$_2$ flat shell elements (510 DOFs) and are applied to the modal analysis of the simply supported cylindrical shell roof. Tab.1 gives the first five frequencies f_i $(i = 1, 2, \cdots, 5)$ solutions of both the 4 BSWI2$_2$ flat shell elements and the other methods [Shen and Wang (1987)]. 4 BSWI2$_2$ calculation results are very high by comparing with the other spline functions methods.

5 Conclusions

A new class of BSWI flat shell element is constructed based on the combination of BSWI plane elastomechanics and Mindlin plate elements. Because the good character of BSWI scaling functions, the element presented in this paper is a useful tool to deal with high performance computation in shell structures especially for folded plate structures. Numerical results verify that the proposed wavelet-based shell element can be utilized to static and dynamic analysis of shell structures easily, similar to the traditional flat shell element. And some advantages of BSWI element in engineering structures analysis have been embodied, i.e. the BSWI elements have higher efficiency and precision than the traditional element.

Because of the good characteristic of BSWI scaling functions, such as multi-resolution analysis and localization, we can choose the higher

Table 2: Comparison of the frequencies between 4 BSWI2_2 elements and the other methods(Hz)

Method	f_1	f_2	f_3	f_4	f_5
Finite strip method	0.284	0.301	0.509	0.527	0.572
Spline FEM	0.2808	0.2999	0.5047	0.5227	0.5710
Spline subdomain method	0.285	0.300	0.507	0.523	0.562
4 BSWI2_2	0.2843	0.301	0.5067	0.5229	0.570

scale BSWIm_j flat shell element easily to deal with higher performance computation in structural analysis. However, it is worth pointed out here that the higher scale BSWIm_j flat shell element might fail to achieve excellent solutions for the error of geometrical approximation for the curved shells.

Acknowledgement: This work was supported by the key project of National Natural Science Foundation of China (No.50335030), National Natural Science Foundation of China(No.50505033), Natural Science Foundation of Guilin University of Electronic Technology (No.Z20701) and Youth Science Foundation of GuangXi province.

References

Atluri, S.N.; Liu, H.T.; Han, Z.D. (2006a): Meshless Local Petrov-Galerkin (MLPG) mixed collocation method for elasticity problems. *CMES: Computer Modeling in Engineering and Sciences*, vol. 14, pp. 141-152.

Atluri, S.N.; Liu, H.T.; Han, Z.D. (2006b): Meshless Local Petrov-Galerkin (MLPG) mixed finite difference method for solid mechanics. *CMES: Computer Modeling in Engineering and Sciences*, vol. 15, pp. 1-16.

Han, Z.D.; Liu, H.T.; Rajendran, A.M.; Atluri, S.N. (2006): The applications of Meshless Local Petrov-Galerkin (MLPG) approaches in high-speed impact, penetration and perforation problems. *CMES: Computer Modeling in Engineering and Sciences*, vol. 14, pp. 119-128.

Parussini, L. (2007): Fictitious domain approach for spectral/hp element method. *CMES: Computer Modeling in Engineering and Sciences*, vol. 17, pp. 95-114.

Cohen, A. (2003): *Numerical Analysis of Wavelet Method*. Elsevier, Amsterdam.

Dahmen, W. (2001): Wavelet methods for PDEs—some recent developments. *Journal of Computational and Applied Mathematics*, vol.128, pp. 133-185.

Canuto, C.; Tabacco, A. and Urban, K. (1999): The wavelet element method part I: construction and analysis. *Applied and Computational Harmonic Analysis*, vol.6, pp. 1-52.

Canuto, C.; Tabacco, A. and Urban, K. (2000): The wavelet element method part II: realization and additional feature in 2D and 3D. *Applied and Computational Harmonic Analysis*, vol.8, pp. 123-165.

Dahlke, S.; Dahmen, W.; Hochmulth, R. et al. (1997): Stable multiscale bases and local error estimation for elliptic problems. *App. Numer Math*, vol. 23, pp. 21-47.

Ko, J.; Kurdila, A. J.; Pilant, M.S. (1995): A class of finite element methods based on orthonormal, compactly supported wavelets. *Computational Mechanics*, vol. 16, pp. 235-244.

Chen, W.H.; Wu, C.W. (1995): A spline wavelets element method for frame structures vibration. *Computational Mechanics*, vol. 16, pp. 11-21.

Chen, W.H.; Wu, C.W. (1996a): Extension of spline wavelets element method to membrane vibration analysis. *Computational Mechanics*, vol. 18, pp. 46-54.

Chen, W.H.; Wu, C.W. (1996b): Adaptable Spline Element for Membrane Vibration Analysis. *Intational Journal for Numerical Methods in Engineering*, vol. 39, pp. 2457-2476.

Zhou, Y.H.; Wang, J.Z.; Zheng, X.J. (1998): Application of wavelet Galerkin FEM to bending of beam and plate structures. *Appl. Math. Mech*,

vol.19, pp.697-706.

Basu, P.K.; Jorge, A.B.; Badri, S. et al. (2003): Higher-order modeling of continua by finite-element, boundary-element, Meshless, and wavelet methods. *Computers and Mathematics with Application*, vol. 46, pp. 15-33.

Ma J.X.; Xue, J.J.; He, Z.J. et al. (2003). A study of the construction and application of a Daubechies wavelet-based beam element. *Finite Element in Analysis and Design*, vol. 39, pp. 965-975.

Chen, X.F.; Yang, S.J.; He, Z.J. et al. (2004): The construction of wavelet finite element and its application. *Finite Element in Analysis and Design*, vol. 40, pp. 541-554.

Han, J.G.; Ren, W.X.; Huang, Y. (2005): A multivariable wavelet-based finite element method and its application to thick plates. *Finite Element in Analysis and Design*, vol. 41, pp. 821-833.

Mitra, M.; Gopalakrishnan, S. (2006): Wavelet based 2-D spectral finite element formulation for wave propagation analysis in isotropic plates. *CMES: Computer Modeling in Engineering and Sciences*, vol. 15, pp. 49-67.

Xiang, J.W.; Chen, X.F.; He ,Y.M.; He, Z.J. (2006a): The Construction of plane elastomechanics and Mindlin plate elements of B-spline wavelet on the interval. *Finite Element in Analysis and Design*, vol. 42, pp. 1269-1280.

Xiang, J.W.; He, Z.J.; Chen, X.F. (2006b): The construction of wavelet-based truncated conical shell element using B-spline wavelet on the interval. *Acta Mechanica Solida Sinica*, vol.19 pp.316-326.

Xiang, J.W.; Chen, X.F.; He, Z.J.; Dong, H.B. (2007): The construction of 1D wavelet finite elements for structural analysis. *Computational Mechanics*, vol. 40, pp. 325-339.

He, Z.J.; Chen, X.F. (2005): Advanced in theory study and engineering application of wavelet finite element. *Chinese Journal of Mechanical Engineering*, vol. 41, pp.1-11.(In Chinese)

Wang, J.Z. (1996): Cubic Spline wavelet bases of Sobolev spaces and multilevel interpolation. *Applied and Computational Harmonic Analysis*, vol. 3, pp. 154-163.

Bertoluzza, S.; Naldi, G.; Ravel, J.C. (1994): Wavelet methods for the numerical solution of boundary value problems on the interval. *Wavelets: Theory, Algorithms, and Applications*. Chui, C.K.; Montefusco, L. and Puccio, L.(eds.). Academic Press, Inc., London, pp.425-448.

Chui, C.K.; Quak, E. (1992): Wavelets on a bounded interval. *Numerical Methods of Approximation Theory*, vol.1, pp. 53-57.

Quak, E.; Weyrichm N. (1994): Decomposition and Reconstruction algorithms for spline wavelets on a Bounded interval. *Applied and Computational Harmonic Analysis*, vol. 3, pp. 217-231.

Goswami, J.C.; Chan, A.K.; Chui, C.K. (1995): On solving first-kind integral equations using wavelets on a bounded interval. *IEEE Transactions on Antennas and Propagation*, vol. 43, pp. 614-622.

Jia, R.Q.; Wang, J.Z.; Zhou, D.X. (2003): Compactly supported wavelet based for Sobolev spaces. *Applied and Computational Harmonic Analysis*, vol. 15, pp. 224-241.

Mallat, S.G. (1999): *A wavelet tour of signal processing* (2^{nd} edition). Academic Press.

Zienkiewicz, O.C.; Taylor, R.L. (1988): *The Finite Element Method* (4^{th} Edition). McGraw-Hill Book Company, London.

Shen, P.C.; Wang, J.G. (1987): Static analysis of cylinder shells by using B-spline functions. *Computers & Structures*, vol. 25, pp. 809-816.